MASS AND RADIUS FORMULAS FOR LOW-MASS NEUTRON STARS

HAJIME SOTANI[1], KEI IIDA[2], KAZUHIRO OYAMATSU[3], AND AKIRA OHNISHI[1]

sotani@yukawa.kyoto-u.ac.jp

Received _____; accepted _____

[1]Yukawa Institute for Theoretical Physics, Kyoto University, Kyoto 606-8502, Japan

[2]Department of Natural Science, Kochi University, 2-5-1 Akebono-cho, Kochi 780-8520, Japan

[3]Department of Human Informatics, Aichi Shukutoku University, 9 Katahira, Nagakute, Aichi 480-1197, Japan

ABSTRACT

Neutron stars, produced at the death of massive stars, are often regarded as giant neutron-rich nuclei. This picture is especially relevant for low-mass (below about solar mass, $M_{\odot}$) neutron stars, where non-nucleonic components are not expected to occur. Due to the saturation property of nucleonic matter, leading to the celebrated liquid-drop picture of atomic nuclei, empirical nuclear masses and radii can be approximately expressed as function of atomic mass number. It is, however, not straightforward to express masses and radii of neutron stars even in the low-mass range where the structure is determined by a balance between the pressure of neutron-rich nucleonic matter and the gravity. Such expressions would be of great use given possible simultaneous mass and radius measurements. Here we successfully construct theoretical formulas for the masses and radii of low-mass neutron stars from various models that are consistent with empirical masses and radii of stable nuclei. In this process, we discover a new equation-of-state parameter that characterizes the structure of low-mass neutron stars. This parameter, which plays a key role in connecting the mass-radius relation of the laboratory nuclei to that of the celestial objects, could be constrained from future observations of low-mass neutron stars.

Subject headings: stars: neutron, equation of state, dense matter

1. INTRODUCTION

Neutron stars have been serving as laboratories to probe the densest and most neutron-rich matter in the Universe. It is generally believed that the outer, low-density part of a neutron star (crust) consists of a body-center-cubic lattice of neutron-rich nuclei, embedded in a gas of electrons and, if any, dripped neutrons, and near normal nuclear density (ρ_0), the nuclei melt into uniform nucleonic matter, which mainly composes the star's core (Lattimer & Prakash 2004). The equation of state (EOS) of matter in the star, i.e., neutron star matter, has one-to-one correspondence to the star's mass (M) and radius (R) relation via hydrostatic equilibrium. Observational data for M have been accumulated (Lattimer & Prakash 2004; Özel et al. 2012; Kiziltan et al. 2013), whereas those for R have been recently estimated from observations of thermonuclear X-ray bursts with photospheric radius expansion and thermal spectra from quiescent low-mass X-ray binaries (Steiner, Lattimer, & Brown 2012; Özel, Baym, & Güver 2010; Guillot et al. 2013; Lattimer & Steiner 2013).

In theoretically describing laboratory nuclei and neutron star matter, it is useful to consider the energy of "nuclear matter," i.e., hypothetical infinite matter, composed of neutrons and of protons that have electric charge switched off. For simplicity, as neutron star matter, we will consider zero-temperature, β equilibrated, charge neutral matter made of real nucleons and electrons. The EOS of nuclear matter can be constrained from terrestrial nuclear experiments (Tsang et al. 2012) and neutron star observations (Özel, Baym, & Güver 2010; Lattimer & Steiner 2013; Demorest et al. 2010) via theoretical calculations. It is noteworthy that the candidates for low-mass neutron stars have been discovered in binary systems (Lattimer & Prakash 2011; Özel et al. 2012), which could give additional information on the EOS once R is measured. We also remark that a strong correlation between the neuron skin thickness of ^{208}Pb and the radius of a $0.5M_{\odot}$ neutron

star was found by Carriere, Horowitz, & Piekarewicz (2003).

The energy of uniform nuclear matter can be expanded around the saturation point of symmetric nuclear matter (SNM), i.e., nuclear matter made of the same number of neutrons and protons, with respect to the nucleon number density, n_b, and neutron excess, α, defined as $\alpha \equiv (n_n - n_p)/n_b$, where n_n and n_p denote the neutron and proton number densities. In practice, in the vicinity of the saturation point of SNM at zero temperature, the energy per nucleon, w, of uniform nuclear matter can be written as a function of n_b and α (Lattimer 1981), i.e.,

$$w = w_0 + \frac{K_0}{18n_0^2}(n_b - n_0)^2 + \left[S_0 + \frac{L}{3n_0}(n_b - n_0)\right]\alpha^2, \tag{1}$$

where w_0, n_0, and K_0 are the saturation energy, the saturation density, and the incompressibility of SNM, while S_0 and L are associated with the symmetry energy coefficient $S(n_b)$. That is, $S_0 = S(n_0)$ is the symmetry energy coefficient at $n_b = n_0$, while L characterizes the density dependence of the nuclear symmetry energy around $n_b = n_0$, defined as $L = 3n_0(dS/dn_b)_{n_b=n_0}$. Among these five parameters in equation (1), the uncertainties in the values of w_0, n_0, and S_0 to be determined from empirical data for masses and radii of stable nuclei are significantly smaller than those in the values of K_0 and L (Oyamatsu & Iida 2003).. This is why we focus on the various sets of K_0 and L (Table 1) in analyzing neutron star matter.

These two parameters, K_0 and L, mainly determine the stiffness of neutron-rich nuclear matter, but have yet to be fixed. It is also suggested that K_0 is related to the giant resonances of stable nuclei (Blaizot 1980), while L is associated with the structure and reactions of neutron-rich nuclei (Tsang et al. 2012; Roca-Maza et al. 2011; Oyamatsu & Iida 2003) and the pressure of pure neutron matter at the saturation density of SNM. Additionally, one could constrain L via quasi-periodic oscillations in giant flares observed from soft-gamma repeaters (Sotani et al. 2012, 2013).

In contrast to the well-known empirical nuclear mass and radius formulas (Blatt & Weisskopf 1952), the neutron star counterparts have to be theoretically given as function of not only the central density (ρ_c), but such EOS parameters as K_0 and L. So far, however, the dependence of low-mass neutron star models on K_0 and L remains to be examined systematically. We thus start with construction of the neutron star models from various EOSs of neutron star matter that meet the following conditions:

1. Unified description of matter in the crust and core based on the same EOS of nuclear matter with specific values of K_0 and L.

2. Consistency of the masses and radii of stable nuclei calculated within the same theoretical framework with the empirical values.

Mass and radius formulas for low-mass neutron stars are finally obtained in such a way as to approximately reproduce the neutron star models thus constructed.

2. ADOPTED EOS'S OF NEUTRON STAR MATTER

Among many available EOSs of neutron star matter, we adopt the EOSs that meet the above conditions, i.e., unified EOSs, which are categorized into three groups as in Table 1. The first is based on the phenomenological EOS of uniform nuclear matter that was constructed by two of us (Oyamatsu & Iida 2003), using a simplified version of the extended Thomas-Fermi theory (Oyamatsu 1993), in such a way as to reproduce empirical masses and radii of stable nuclei. They adopted the Padé-type potential energies with respect to the nucleon density n_b for SNM and for neutron matter, respectively, and connected them in a quadratic approximation with respect to neutron excess α. This form of the potential energy can well reproduce the variational calculations of Friedman & Pandharipande (1981), to which, in fact, the high-density behavior of neutron matter was adjusted. The

α dependence of the potential energy is partially justified by the variational calculations of Lagaris & Pandharipande (1981), and the expression for the total energy reproduces equation (1) in the limit of $n_b \to n_0$ and $\alpha \to 0$. With such EOSs of uniform nuclear matter obtained for various sets of (K_0, L), they constructed the EOSs of neutron star matter (Oyamatsu & Iida 2007) by generalizing the above Thomas-Fermi theory as done by Oyamatsu (1993). The resultant EOSs are referred to as the OI-EOSs. We remark that as shown in Table 1, the corresponding K_0 values contain extreme cases (OI 180 and OI 360).

In the second group, there are two EOSs of neutron star matter calculated within the relativistic framework. One is the Shen EOS based on the relativistic mean field theory with the TM1 nuclear interaction (Shen et al. 1998), and the other is the Miyatsu EOS based on the relativistic Hartree-Fock theory with the chiral quark-meson coupling model (Miyatsu, Yamamuro, & Nakazato 2013). In both EOSs, the same type of the Thomas-Fermi model as used for the OI-EOSs is used in describing neutron star matter in such a way as to reproduce empirical masses and radii of stable nuclei.

The third group is composed of the five EOSs of neutron star matter based on the Skyrme-type effective interactions: FPS (Lorenz, Ravenhall, & Pethick 1993), SLy4 (Douchin & Haensel 2001), BSk19, BSk20, and BSk21 (Goriely, Chamel, & Pearson 2010; Pearson, Goriely, & Chamel 2011; Pearson et al. 2012). The FPS interaction, which was constructed by fitting the properties of uniform nucleon matter calculated by Friedman & Pandharipande (1981), well reproduces the empirical ground-state properties of doubly magic stable nuclei via the Hartree-Fock calculations. The SLy4 interaction was constructed by Chabanat et al. (1997) in such a way as to reproduce the microscopic EOS of neutron matter calculated with the UV14+UVII nuclear force by Wiringa, Fiks, & Fabrocini (1998) as well as the empirical ground-state properties of doubly magic stable nuclei within the Hartree-Fock approximation. The BSk19, BSk20, and

BSk21 interactions are written in the form of the nuclear energy-density functionals, which are derived from generalized Skyrme interactions in such a way as to fit all the available nuclear mass data (Goriely, Chamel, & Pearson 2010). As a result, empirical charge radii were also well reproduced. These interactions are different in the sense that BSk19, BSk20, and BSk21 are fitted to the EOSs of neutron matter derived by Friedman & Pandharipande (1981), Akmal, Pandharipande, & Ravenhall (1998), and Li & Schulze (2008), respectively. This difference is expected to play a role in estimating the effect of uncertainties in three-neutron interactions on the stellar properties, as we shall see. In describing neutron star matter, a compressible liquid-drop approach was used for FPS and SLy4, while an extended Thomas-Fermi model was used for BSk19, BSk20 and BSk21. To calculate the neutron star models in the present study, we adopt the analytical expressions for FPS and SLy4 given by Haensel & Potekhin (2004) and for BSk19, BSk20, and BSk21 given by Potekhin et al. (2013).

We conclude this section by mentioning that a strong correlation between S_0 and L is known from empirical nuclear masses and radii (Oyamatsu & Iida 2003; Lattimer & Lim 2013). In order to check whether or not a similar correlation appears in the EOS models adopted here, we plot in Figure 1 L vs. S_0 by using the values listed in Table 1. We thus see a good agreement with the linear correlation obtained by Oyamatsu & Iida (2003) in such a way as to reproduce empirical masses and radii for stable nuclei [1].

[1]Recently, Newton, Gearheart, & Li (2013) systematically examined the properties of the neutron star inner crust by changing the values of S_0 and L with reference to such a S_0-L relation as shown in Figure 1, while keeping K_0 fixed.

3. NEUTRON STAR MODELS

Now, we construct nonrotating neutron stars by integrating the Tolman-Oppenheimer-Volkoff equations from the stellar center of density ρ_c outward up to the position where the pressure vanishes. It is not clear up to what density the adopted unified EOSs are applicable. Nonetheless, one can expect that non-nucleonic components such as hyperons and quarks do not occur below $\sim 2\rho_0$ (Lattimer & Prakash 2004) and that the uncertainty from three-neutron interactions in the EOS of pure neutron matter becomes relevant above $\sim 2\rho_0$, as suggested by quantum Monte Carlo (QMC) calculations (Gandolfi, Carlson, & Reddy 2012). We thus examine the stellar models for $\rho_c \leq 2\rho_0$, where ρ_0 is set to 2.68×10^{14} g cm^{-3}, and the resultant M-R relations are plotted in Figure 2(a).

To systematically describe various stellar models, we introduce a new auxiliary parameter η defined as $\eta = (K_0 L^2)^{1/3}$. The values of η are shown in Table 1. Remarkably, the M-R relation changes almost smoothly with η. Note that the OI-EOSs (Oyamatsu & Iida 2007) with $L \lesssim 10$ MeV are too soft to keep the pressure positive and thus not used here. This implies the lower limit of η of order 30 MeV. Meanwhile, the EOS models used here cover the values of η up to ~ 200 MeV, which is significantly larger than expected from existing nuclear experiments.

From the observational viewpoint, the radiation radius $R_\infty = R/\sqrt{1-2GM/Rc^2}$ and the gravitational redshift $z = 1/\sqrt{1-2GM/Rc^2} - 1$ with the gravitational constant G and the speed of light c could be more relevant in describing the stellar properties than M and R. The calculated z-R_∞ relation again shows a smooth change with η (Figure 2(b)). The photon flux, if detected, would be proportional to $(R_\infty/D)^2$, where D is the distance from the Earth, while the gravitational redshift could be determined from the possible shift of atomic absorption lines in spectra of the stars.

The smooth change of the stellar properties with η suggests that not only future

nuclear experiments but also simultaneous measurements of M and R or, equivalently, z and R_∞ could constrain η, which could in turn lead to restriction of the stellar models. In particular, observations of low-mass neutron stars would be essential. For example, the radiation radius of the X-ray source, CXOU 132619.7–472910.8, in the globular cluster NGC 5139 (ω Cen) has been determined as $R_\infty = 14.3 \pm 2.1$ km from the *Chandra* data (Rutledge et al. 2002). The allowed region from this R_∞ is shown in Figure 2(a) and (b) with the shaded region. This is still consistent with various values of η, but future precise determination of R_∞ could constrain η, if M is low enough. Additionally, thermal spectra detected from quiescent low-mass X-ray binaries are expected to give M and R simultaneously (Guillot et al. 2013; Lattimer & Steiner 2013).

4. MASS AND RADIUS FORMULAS

To examine the dependence of the stellar properties on η more clearly, we plot the stellar masses calculated for $\rho_c = 2.0\rho_0$, $1.5\rho_0$, and $1.0\rho_0$ (Figure 3(a)). From this figure, we find that the stellar masses for fixed ρ_c can be approximately expressed as a linear function of η, $M/M_\odot = c_0 + c_1(\eta/100\,\mathrm{MeV})$, where c_0 and c_1 are adjustable parameters that depend on ρ_c [2]. The validity of η is now evident. The deviation of the calculations from the linear fit at $\rho_c = 2.0\rho_0$ is larger than that at $\rho_c = 1.0\rho_0$, particularly for BSk20 and BSk21. Such deviation is of the order of uncertainties in M due to three-neutron interactions obtained from the QMC evaluations (Gandolfi, Carlson, & Reddy 2012). The parameters c_0 and c_1 can then be expressed as a quadratic function of $u_c \equiv \rho_c/\rho_0$ within the accuracy of errors

[2]Even if we perform the fitting by excluding OI 180 and OI 360 in which case K_0 is rather extreme, the fitting lines almost overlap those shown in Figure 3(a).

less than a few percent (Figure 4). Finally, we obtain the mass formula:

$$\frac{M}{M_\odot} = 0.371 - 0.820u_c + 0.279u_c^2 - (0.593 - 1.25u_c + 0.235u_c^2)\left(\frac{\eta}{100\,\mathrm{MeV}}\right), \qquad (2)$$

where we confine ourselves to $\rho_c \gtrsim 0.9\rho_0$; otherwise, the stellar models can become unstable with respect to decompression, depending on the EOS of neutron star matter. To examine the validity of this mass formula, we evaluate the relative root-mean-square deviations of the formula values from the original values obtained from the EOSs adopted here. The results are 3.55%, 1.76%, and 4.74% for $\rho_c = 2.0\rho_0$, $1.5\rho_0$, and $1.0\rho_0$, respectively, which are fairly small.

We also find that the gravitational redshift calculated for fixed ρ_c can be approximately expressed as a linear function of η (Figure 3(b)) [3]. Then, just like the mass formula (2), we can obtain the theoretical formula for z as

$$z = 0.00859 - 0.0619u_c + 0.0255u_c^2 - (0.0429 - 0.108u_c + 0.0120u_c^2)\left(\frac{\eta}{100\,\mathrm{MeV}}\right), \qquad (3)$$

which leads to the relative root-mean-square deviations from the original values: 4.54%, 2.80%, and 5.31% for $\rho_c = 2.0\rho_0$, $1.5\rho_0$, and $1.0\rho_0$.

It is straightforward to obtain the formula for R from equations (2) and (3). The obtained formula can be compared with the calculations of R for $\rho_c = 1.0\rho_0$, $1.5\rho_0$, and $2.0\rho_0$ (Figure 5). We confirm a good agreement between those two except for $\eta \lesssim 70$ MeV. The mass and radius formulas could help to constrain not only the nuclear matter parameter η but also a star's ρ_c via possible simultaneous measurements of the star's M and R. If such measurements are precise, η could be deduced to within the accuracy of ± 20 MeV, which would provide a basis for analyzing more massive neutron stars.

[3]Again, the fitting lines that have the results with OI 180 and OI 360 excluded almost overlap those lines in Figure 3(b).

From Figure 5, one can also observe that the calculated R depends nonlinearly on ρ_c at small values of η, while converging on an approximately linear function of η at sufficiently large values of η:

$$R = 10.32 + 2.57 \left(\frac{\eta}{100\,\mathrm{MeV}} \right) \text{ km}. \tag{4}$$

Note that this convergence is related to the straightened behavior of the M-R relations that can be seen from Figure 2(a).

5. CONCLUSION

In this paper, we have succeeded in constructing the theoretical formulas for the masses, gravitational redshifts, and radii of low-mass neutron stars as functions of the star's central density and the new EOS parameter η in a manner that is consistent with empirical masses and radii of stable nuclei. The value of η, which characterizes the stiffness of neutron star matter, remains unknown, but could be deduced from possible simultaneous M and R measurements via comparison with our formulas if the star observed is light enough. Thus, a firm evidence for the presence of low-mass neutron stars is first of all desired. One promising candidate is the neutron star in the high-mass X-ray binary 4U 1538-52, of which the mass could be significantly low or even the lowest among stars with known mass if the binary orbit is eccentric (Rawls et al. 2011; Petrov, Antokhina, & Cherepashchuk 2013). The X-ray burster 4U 1724-307 in the globular cluster Terzan 2 is even more interesting because the X-ray data from the cooling phase of photospheric radius expansion bursts apparently allow the object to have a relatively low mass and still a significantly large radius (Suleimanov et al. 2011). Such conclusions are tentative partly because of the dependence on the atmosphere models adopted and partly because of uncertainties in the distance to the object, but, if valid, might eventually suggest the η value of order or even larger than 130 MeV.

H.S. is grateful to C. Ishizuka, K. Sumiyoshi, T. Tatsumi, and N. Yasutake for comments. H.S., K.I., and A.O. acknowledge the hospitality of the Facility for Rare Isotope Beams, where this work was initiated, and thank T. Enoto for helpful discussions. This work was supported in part by Grants-in-Aid for Scientific Research on Innovative Areas through No. 24105001 and No. 24105008 provided by MEXT, in part by Grant-in-Aid for Young Scientists (B) through No. 24740177 provided by JSPS, in part by the Yukawa International Program for Quark-hadron Sciences, and in part by Grant-in-Aid for the global COE program "The Next Generation of Physics, Spun from Universality and Emergence" from MEXT.

REFERENCES

Akmal, A., Pandharipande, V. R., & Ravenhall, D. G. 1998, Phys. Rev. C, 58, 1804

Blaizot, J. P. 1980, Phys. Rep., 64, 171

Blatt, J. M. & Weisskopf, V. F. 1952, Theoretical Nuclear Physics (New York: Wiley)

Carriere, J., Horowitz, C. J., & Piekarewicz, J. 2003, ApJ, 593, 463

Chabanat, E., Bonche, P., Haensel, P., Meyer, J., & Schaeffer, R. 1997, Nucl. Phys. A, 627, 710

Demorest, P. B., Pennucci, T., Ransom, S. M., Roberts, M. S. E., & Hessels, J. W. T. 2010, Nature, 467, 1081

Douchin, F. & Haensel, P. 2001, A&A, 380, 151

Friedman, B. & Pandharipande, V. R. 1981, Nucl. Phys. A, 361, 502

Gandolfi, S., Carlson, J., & Reddy, S. 2012, Phys. Rev. C, 85, 032801

Goriely, S., Chamel, N., & Pearson, J. M. 2010, Phys. Rev. C, 82, 035804

Guillot, S., Servillat, M., Webb, N. A., & Rutledge, R. E. 2013, ApJ, 772, 7

Haensel, P. & Potekhin, A. Y. 2004, A&A, 428, 191

Kiziltan, B., Kottas, A., De Yoreo, M., & Thorsett, S. E. 2013, ApJ, 778, 66

Lagaris, I. E. & Pandharipande, V. R. 1981, Nucl. Phys. A, 369, 470

Lattimer, J. M. 1981, Annu. Rev. Nucl. Part. Sci., 31, 337

Lattimer, J. M. & Prakash, M. 2004, Science, 304, 536

Lattimer, J. M. & Prakash, M. 2011, in From Nuclei to Stars: Festschrift in Honor of Gerald E Brown, ed. S. Lee (Singapore: World Scientific), 275

Lattimer, J. M. & Lim, Y. 2013, ApJ, 771, 51

Lattimer, J. M. & Steiner, A. W. 2013, arXiv:1305.3242

Li, Z. H. & Schulze, H. J. 2008, Phys. Rev. C, 78, 028801

Lorenz, C. P., Ravenhall, D. G., & Pethick, C. J. 1993, Phys. Rev. Lett., 70, 379

Miyatsu, T., Yamamuro, S., & Nakazato, K. 2013, ApJ, 777, 4

Newton, W. G., Gearheart, M., & Li, B. A. 2013, ApJS, 204, 9

Oyamatsu, K. 1993, Nucl. Phys. A, 561, 431

Oyamatsu, K. & Iida, K. 2003, Prog. Theor. Phys., 109, 631

Oyamatsu, K. & Iida, K. 2007, Phys. Rev. C, 75, 015801

Özel, F., Baym, G., & Güver, T. 2010, Phys. Rev. D, 82, 101301

Özel, F., Psaltis, D., Narayan, R., & Villarreal, A. S. 2012, ApJ, 757, 55

Pearson, J. M., Goriely, S., & Chamel, N. 2011, Phys. Rev. C, 83, 065810

Pearson, J. M., Chamel, N., Goriely, S., & Ducoin, C. 2012, Phys. Rev. C, 85, 065803

Petrov, V. S., Antokhina, E. A., & Cherepashchuk, A. M. 2013, Astron. Rep., 57, 669

Potekhin, A. Y., Fantina, A. F., Chamel, N., Pearson, J. M., & Goriely, S. 2013, A&A, in press (arXiv:1310.0049)

Rawls, M. L. et al. 2011, ApJ, 730, 25

Roca-Maza, X., Centelles, M., Viñas, X., & Warda, M. 2011, Phys. Rev. Lett., 106, 25250

Rutledge, R. E., Bildsten, L., Brown, E. F., Pavlov, G. G., & Zavlin, V. E. 2002, ApJ, 578, 405

Shen, H., Toki, H., Oyamatsu, K., & Sumiyoshi, K. 1998, Nucl. Phys. A, 637, 435

Sotani, H., Nakazato, K., Iida, K., & Oyamatsu, K. 2012, Phys. Rev. Lett., 108, 201101

Sotani, H., Nakazato, K., Iida, K., & Oyamatsu, K. 2013, MNRAS, 428, L21

Steiner, A. W., Lattimer, J. M., & Brown, E. F. 2013, ApJ, 765, L5

Suleimanov, V., Poutanen, J., Revnivtsev, M., & Werner, K. 2011, ApJ, 742, 122

Tsang, M. B. et al. 2009, Phys. Rev. Lett., 102, 122701

Tsang, M. B. et al. 2012, Phys. Rev. C, 86, 015803

Wiringa, R. B., Fiks, V., & Fabrocini, A. 1988, Phys. Rev. C, 38, 1010

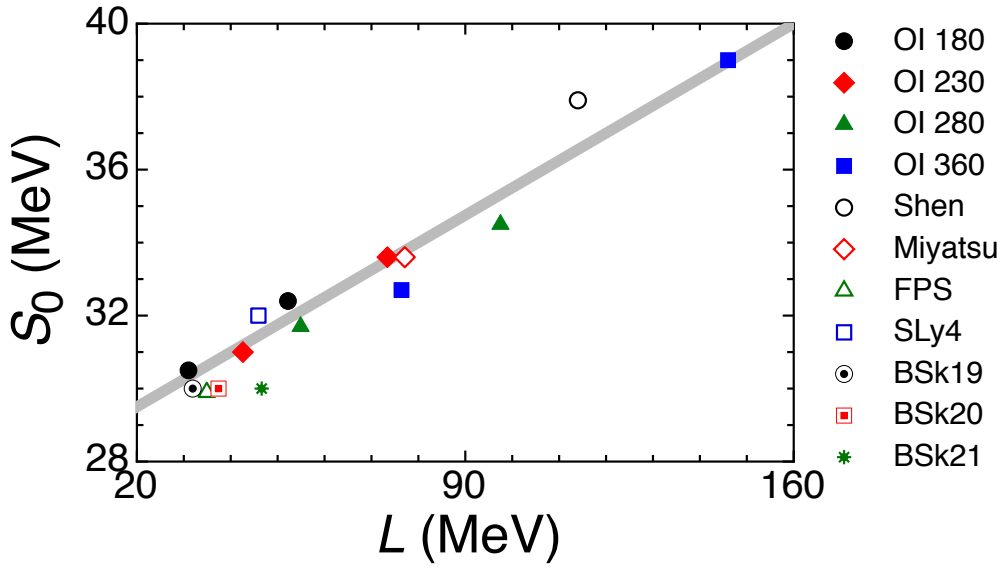

Fig. 1.— Relationship between L and S_0 for various unified EOSs adopted in this paper. The solid line denotes the linear correlation found by Oyamatsu & Iida (2003). (A color version of this figure is available in the online journal.)

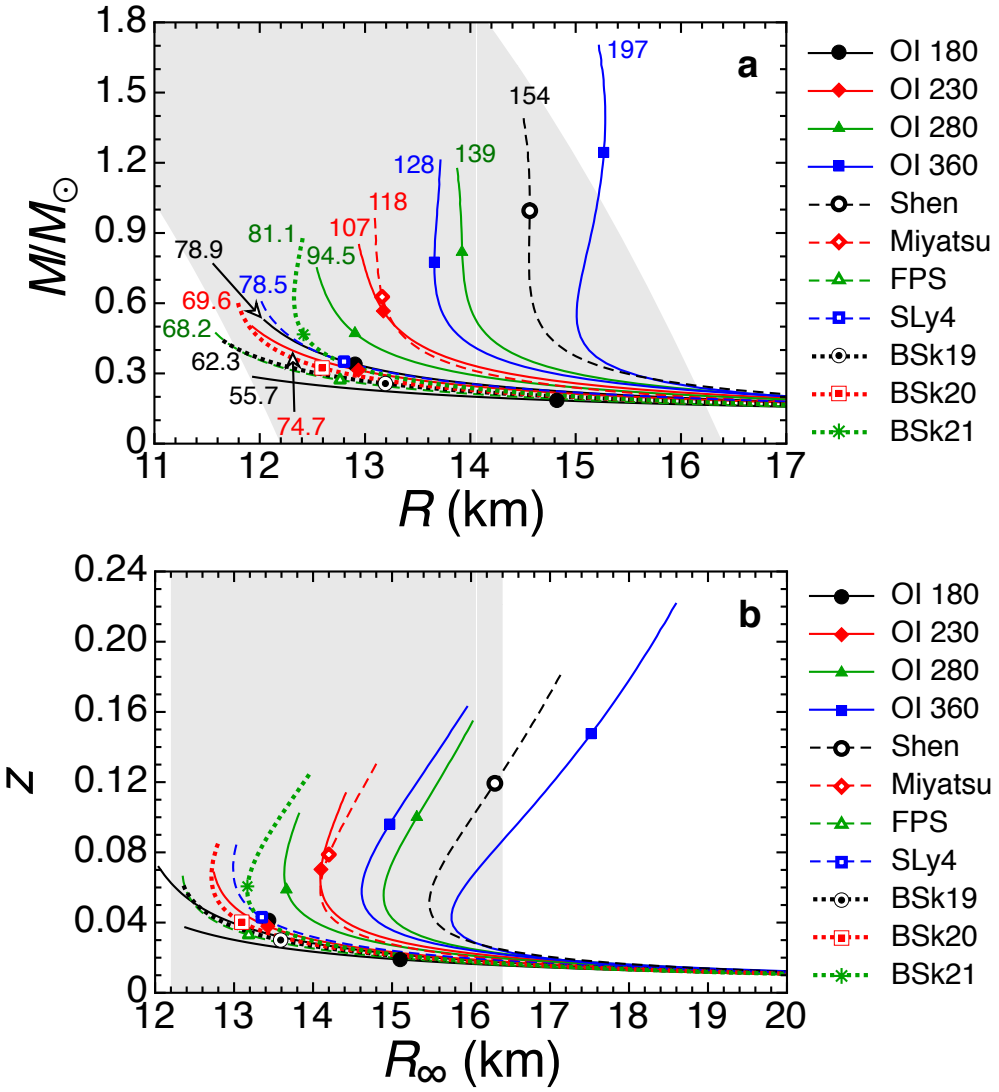

Fig. 2.— Neutron star properties. The stellar models are constructed from various unified EOSs with different sets of (L, K_0). We plot the relations between the mass and radius (a) and between the gravitational redshift and radiation radius (b). The mark and end on each line denote the stellar models with $\rho_c = 1.5\rho_0$ and $2.0\rho_0$, respectively. In (a), the labels on the lines denote the values of the nuclear matter parameter η. To distinguish between the OI-EOSs, we add the values of K_0 to the OI-EOS labels; for example, we use "OI 180" for the two OI-EOSs with $K_0 = 180$ MeV (left, smaller L; right, larger L). The shaded region corresponds to the allowed region from the observed radiation radius of the neutron star in ω Cen (see text for details). (A color version of this figure is available in the online journal.)

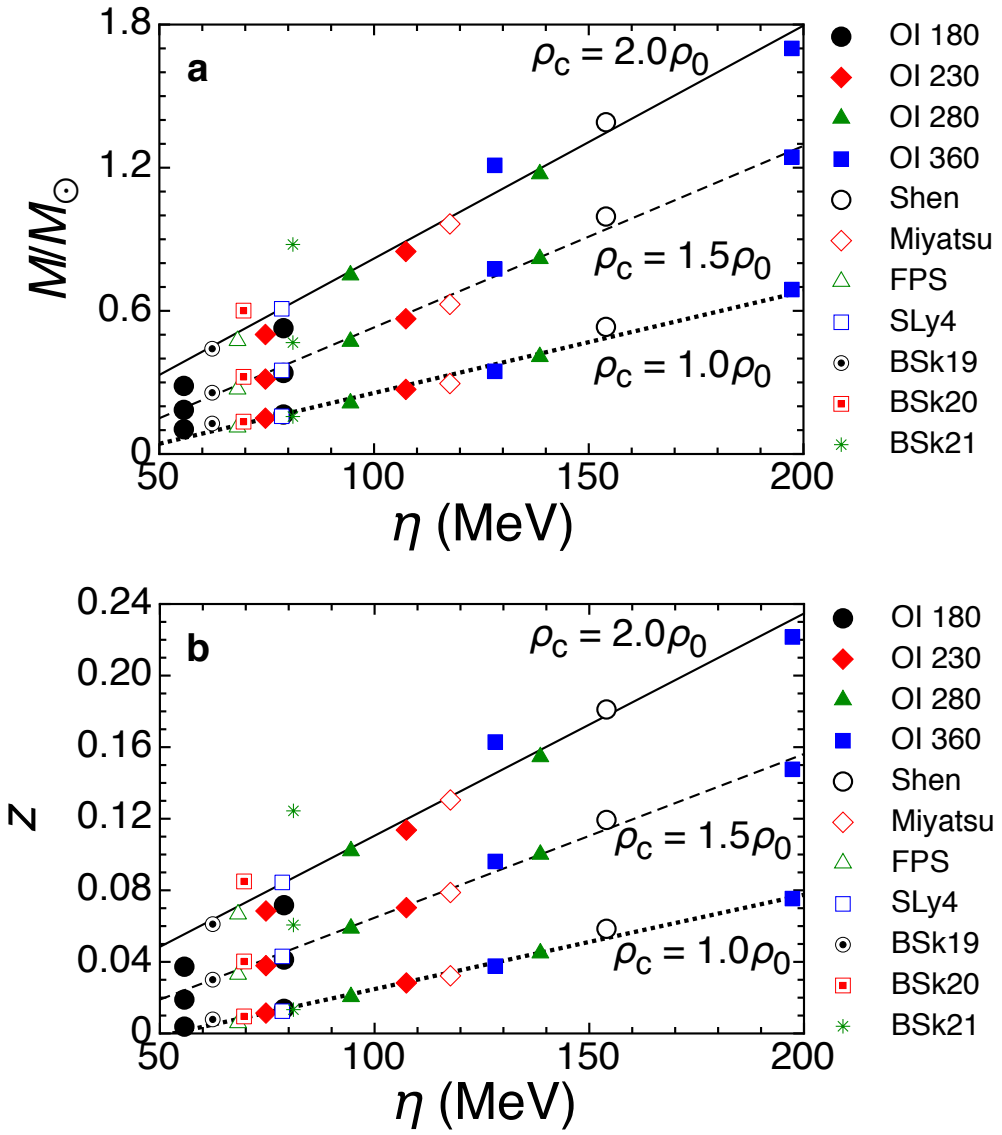

Fig. 3.— Neutron star masses (a) and gravitational redshifts (b) as a function of η. The stellar models constructed from various unified EOSs are given for $\rho_c = 2.0\rho_0$, $1.5\rho_0$, and $1.0\rho_0$. The solid, broken and dotted lines are the linear fitting to the cases of $\rho_c = 2.0\rho_0$, $1.5\rho_0$, and $1.0\rho_0$, respectively (see text for details). (A color version of this figure is available in the online journal.)

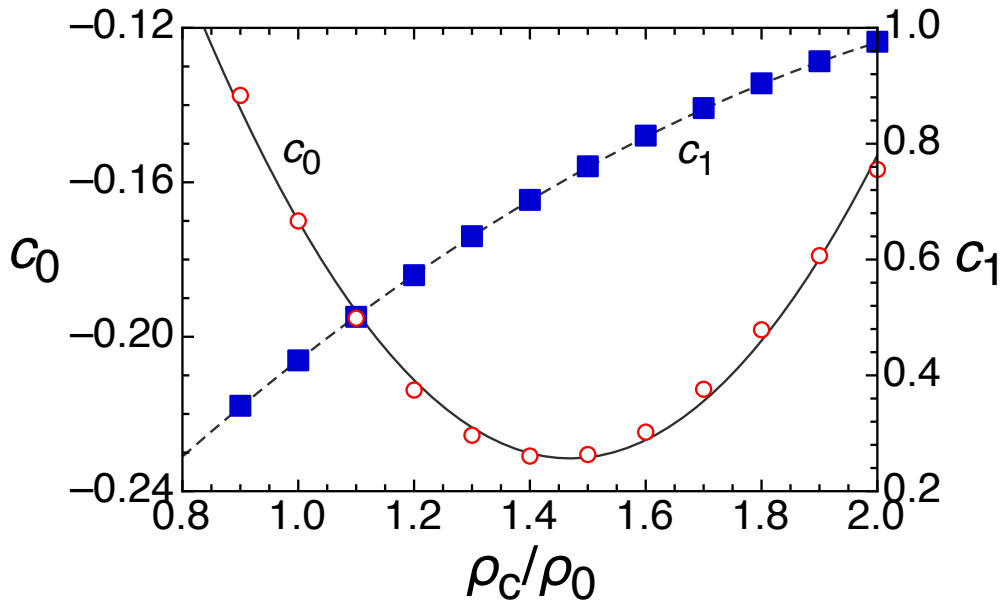

Fig. 4.— Values (marks) of the adjustable parameters c_0 and c_1 in the mass formula. The corresponding quadratic fitting curves (solid and broken lines) are also shown as a function of ρ_c/ρ_0. Here we consider the stellar models only for $\rho_c \gtrsim 0.9\rho_0$ to avoid unstable neutron star models. (A color version of this figure is available in the online journal.)

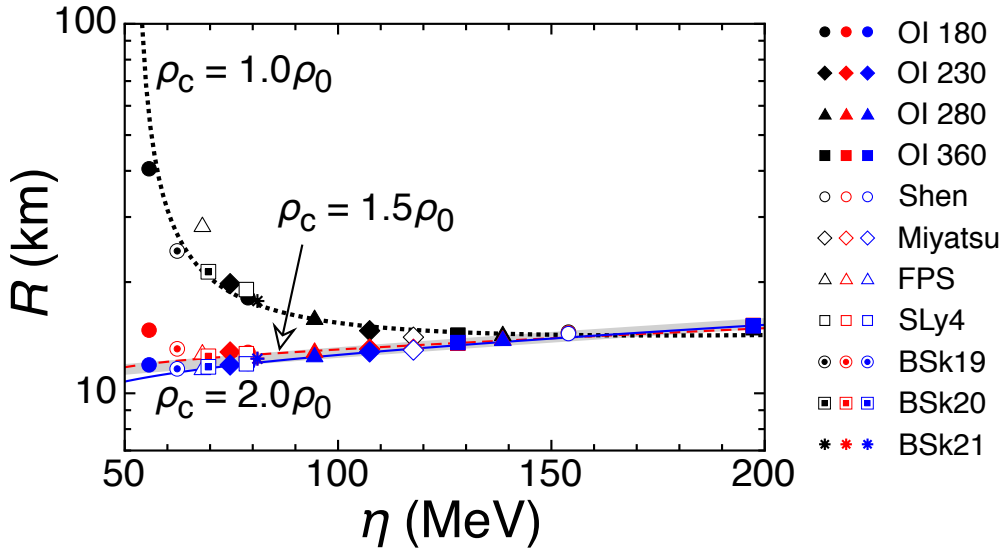

Fig. 5.— Neutron star radii as a function of η. The stellar models constructed from various unified EOSs are given for $\rho_c = 1.0\rho_0$ (black), $1.5\rho_0$ (red), and $2.0\rho_0$ (blue). The solid, broken and dotted lines are the the formula values for the cases of $\rho_c = 2.0\rho_0$, $1.5\rho_0$, and $1.0\rho_0$, respectively, obtained from equations (2) and (3). The thick straight line denotes the converging behavior expressed by equation (4).

Table 1: Nuclear Matter EOS Parameters

EOS	K_0 (MeV)	L (MeV)	S_0 (MeV)	η (MeV)
OI-EOSs	180	31.0	30.5	55.7
	180	52.2	32.4	78.9
	230	42.6	31.0	74.7
	230	73.4	33.6	107
	280	54.9	31.7	94.5
	280	97.5	34.5	139
	360	76.4	32.7	128
	360	146	39.0	197
Shen	281	114	37.9	154
Miyatsu	274	77.1	33.6	118
FPS	261	34.9	29.9	68.2
SLy4	230	45.9	32.0	78.5
BSk19	237	31.9	30.0	62.3
BSk20	241	37.4	30.0	69.6
BSk21	246	46.6	30.0	81.1